Hourglass Pore-Forming Domains Restrict Aquaporin-1 Tetramer Assembly†

John C. Mathai and Peter Agre*

Departments of Biological Chemistry and Medicine, Johns Hopkins University School of Medicine, Baltimore, Maryland 21205

Received October 2, 1998; Revised Manuscript Received November 18, 1998

ABSTRACT: The AQP1 water channel protein is a homotetramer with 28 kDa subunits containing six transmembrane domains. The sequence-related loops B (cytoplasmic) and E (extracellular) were predicted to overlap within the membrane, forming an aqueous pore ("the hourglass") flanked by the corresponding B and E residues 73 and 189. Cryoelectron microscopy of AQP1 previously revealed the central hourglass structure surrounded by six transmembrane helices which provide contact points between subunits. Several mutants in loop B and E residues were nonfunctional when expressed in *X. laevis* oocytes, but their ability to form tetramers is unknown. To explore the possible functional dependence of hourglass domains in adjacent subunits, we prepared a series of tandem dimers as single 55 kDa polypeptides containing different combinations of wild-type (AQP1) or mutant subunits (A73M or C189M). In oocytes, AQP1−AQP1 exhibited high osmotic water permeability, and AQP1−C189M exhibited half activity. Dimer polypeptides with A73M were nonfunctional or not expressed. In yeast secretory vesicles, AQP1−AQP1 exhibited high water permeability, AQP1−C189M exhibited half activity, and both were inhibited by pCMBS. Although expressed, the dimer polypeptides with A73M were all nonfunctional. Tetramer formation was investigated by detergent solubilization and velocity sedimentation through sucrose gradients. Dimer polypeptides containing one A73M subunit or two C189M subunits migrated with slower velocity (s < 3.5 S). In contrast, dimer polypeptides with one C189M subunit migrated with velocity similar to native AQP1 tetramers ($s \sim 6$ S). Thus, although hourglass pore-forming domains are not points of subunit−subunit contact, the structure of loop B is important to normal tetramer assembly.

The existence of water pores was predicted to explain the rapid movements of water across cell membranes during osmosis (*1*). The high water permeability characteristic of red cells, renal proximal tubules, and certain other tissues is now known to be due to the presence of AQP1[1] water channel proteins in the plasma membranes of these cells (*2*−*5*). AQP1 is a 28 kDa integral membrane protein with high selectivity for water and low activation energy (<5 kcal/mol) which is inhibited by $HgCl_2$ and organomercurial pCMBS (*6, 7*). Since discovery of AQP1, numerous mammalian, plant, yeast, and bacterial water channels have been cloned and characterized (*8*).

Considerable insight into the structure of AQP1 has been achieved. The primary amino acid sequence of AQP1 revealed that the N- and C-terminal halves of the protein represent two tandem sequence repeats, each comprised of three bilayer-spanning domains with two connecting loops (*9*). The most highly conserved sequences are present in loop B (cytoplasmic) and loop E (extracellular) which each contain the signature motif Asn-Pro-Ala (NPA) (*10*). The Hg^{2+}-sensitive site Cys-189 resides in loop E preceding the NPA motif, and this residue is believed to lie near a critical narrowing of the aqueous pathway (*11, 12*).

A functionally relevant structural model has been proposed and is being confirmed by physical studies of AQP1 protein. The tandem repeats within AQP1 are oriented to each other in obverse symmetry (*13*). The mutant C189S is water permeable but is not sensitive to Hg^{2+} inhibition, while C189M is not functional. Ala-73 in loop B corresponds to residue 189 in loop E, and expression in oocytes of the double mutant A73C/C189S results in water permeability which is inhibited by Hg^{2+} (*14*). Thus, residues 73 and 189 are functionally similar with respect to water permeation. From this, it was predicted that loop B and loop E overlap between the leaflets of the bilayer, forming a continuous aqueous pathway referred to as the "hourglass"(*14*). Cryoelectron microscopic studies of membrane crystals showed at 6 Å resolution that each AQP1 subunit has six tilted, bilayer-spanning helices surrounding a central area most likely formed by loops B and E which carry the highly conserved residues involved in water permeation (*15*−*17*).

AQP1 exists as a homotetramer (*3, 15, 18*). It is not known with certainty if each subunit contains a single central pore, if pores exist in spaces between subunits, or if the subunits interact functionally. Expression of cDNA dimer constructs encoding 55 kDa polypeptides with two tandem wild-type subunits (AQP1−AQP1), two Hg^{2+}-insensitive subunits (C189S−C189S), or hybrid dimers (AQP1−C189S, C189S−AQP1) resulted in water permeability of full, negligible, or

† Supported by a Postdoctoral Fellowship from the American Heart Association, Maryland Affiliate (to J.C.M.), and by NIH Grants HL33991, HL48268, and EY11239 (to P.A.).

* Corresponding author: Department of Biological Chemistry, Johns Hopkins University School of Medicine, 725 N. Wolfe St., Baltimore, MD 21205-2185. E-mail: pagre@bs.jhmi.edu. Fax: 410-955-3149. Telephone: 410-955-7049.

[1] Abbreviations: P_f, coefficient of osmotic water permeability (cm/s); AQP1, aquaporin-1; CHAPS, 3-[(3-cholamidopropyl)dimethylammonio]-1-propanesulfonate; pCMBS, *p*-(chloromercuri)benzenesulfonate; PAGE, polyacrylamide gel electrophoresis.

10.1021/bi9823683 CCC: $18.00
Published on Web 12/29/1998

intermediate sensitivity to Hg^{2+} (*14, 19*). Attempts to demonstrate hetero-oligomeric composition of AQP1 tetramers by injecting two different cRNAs into oocytes revealed that coexpression of the inactive mutant C189M and the inactive truncation mutant D237Z resulted in a functional complementation, whereas the inactive mutant A73M failed to complement either mutant. Thus, residues 73 and 189 apparently contribute differently to the overall AQP1 structure, possibly due to distinct contributions to subunit−subunit associations.

Interpretation of mutant forms of AQP1 expressed in oocytes is often made difficult by failure of the polypeptides to traffic to the plasma membrane (*11*). Although presumed to reflect abnormalities in protein folding, mutant forms of AQP1 have never been reported to result from defective tetramer assembly. Expression of mammalian aquaporins has been achieved in yeast vesicles (*20*), and this permitted functional analysis of a mutant insect aquaporin which was not possible in oocytes (*21*). Here we employed the yeast vesicle system to evaluate tandem dimers containing different combinations of wild-type (AQP1) or mutant subunits (A73M, C189M) to evaluate whether hourglass pore-forming domains may perturb interactions between adjacent subunits. While residues 73 and 189 are functionally similar during water permeation and are not points of subunit−subunit contact, our results demonstrate that these residues contribute to tetramer assembly, and the loop B residue 73 is more critical than loop E residue 189 to oligomerization.

MATERIALS AND METHODS

Materials. Polyclonal, affinity-purified rabbit antibodies were previously described (*3*). Anti-rabbit IgG was from Boehringer Mannheim; enhanced chemiluminescence reagents were from Amersham; electrophoresis reagents were from Bio-Rad. pYES2 vector was obtained from Invitrogen; SY1 yeast strain and pPMA1.2 plasmid containing the 700 bp 3′ untranslated region of yeast ATPase gene were a gift from Dr. Rajini Rao, Johns Hopkins School of Medicine.

AQP1 Dimer Constructs. Mutant dimers of AQP1 were generated in pBlueScript II KS^- (pBSII) as described previously for the wild-type AQP1 dimer construct (*14*). For expression in yeast, unique *Hin*dIII and *Acc*I sites were added to the 5′ and 3′ ends of the wild-type and mutant AQP1 dimers by PCR with appropriate oligonucleotide primers. A 700 bp fragment containing the 3′ untranslated region of the yeast ATPase gene was cut from PMA1.2 with *Acc*I and *Bam*HI and ligated into pBSII. The PCR products were digested with *Hin*dIII and *Acc*I and ligated into the same sites of the pBSII construct. The resulting plasmid was then digested with *Hin*dIII and *Xba*I. The fragment containing the AQP1 dimer and ATPase sequence was purified and ligated into the same sites in pYES2 for expression in yeast.

Preparation of Oocytes and Measurement of P_f. Capped RNA transcripts were synthesized in vitro (*11*). Stage V and VI oocytes from *X. laevis* were injected with either 50 nL of 1−10 ng of RNA in water or 50 nL of water. Oocytes were maintained at 18 °C for 2−3 days in modified Barth's solution prior to osmotic water permeability measurements. Osmotic water permeability was measured by videomicroscopically monitoring changes in oocyte volume after transfer from 200 mosM isotonic medium to 70 mosM hypotonic medium at 22 °C (*11*). Coefficients of osmotic water permeability (P_f, cm/s) were calculated from swelling data between 15 and 30 s, initial oocyte volume ($V_0 = 9 \times 10^{-4}$ cm^3), initial oocyte surface area ($S = 0.045$ cm^2), and the molar volume of water ($V_w = 18$ cm^3/mol) (*22*):

$$P_f = [V_0 d(V/V_0)/dt]/[SV_w(osm_{in} - osm_{out})]$$

Oocyte Membrane Preparation and Immunoblot Analysis. Oocyte plasma membranes were isolated from groups of 10−15 oocytes (*23*) and solubilized in 1.25% (w/v) SDS, electrophoresed into a 12% SDS−polyacrylamide gel (*24*), and transferred to nitrocellulose membranes (*25*) which were incubated with a 1:1000 dilution of affinity-purified anti-AQP1 (*2, 3*) and visualized by enhanced chemiluminescence.

Yeast Strains and Growth Conditions. Temperature-sensitive SY1 strains of *S. cerevisiae* were used (*MATa, ura3−52, leu2−3,112, his4−619, sec6−4, GAL*)(*26*). Yeast containing various plasmids were grown and maintained on defined minimal medum [yeast nitrogen base, 6.7 g/L (Bio 101; Vista, CA), 20 mg/L histidine, 30 mg/L leucine, 2% glucose as the carbon source]. One liter of yeast culture was grown at room temperature to mid-log phase ($OD_{600} \sim 1$), and cells were harvested by centrifugation at 2000*g* for 10 min at room temperature. Production of AQP1 and accumulation of secretory vesicles were induced by transfer to 1 L of rich YEP-galactose medium [0.5% yeast extract, 1% bactopeptone (Difco Labs, Detroit, MI), 2% galactose (w/v)] during overnight incubation at 37 °C. Sodium azide (10 mM) was added to the cells 10 min prior to harvesting them by centrifugation.

Spheroplast Preparation and Secretory Vesicle Isolation. Yeast cells are suspended at a density of 50 OD_{600} units/mL in spheroplasting medium (1.4 M sorbitol, 50 mM Tris-HCl, pH 7.5, 40 mM β-mercaptoethanol, and 10 mM sodium azide) containing lyticase at 0.2 mg/mL, and incubated at 37 °C for 45 min. Spheroplast are collected by low-speed centrifugation (1000*g* for 15 min at 4 °C) and resuspended in the same volume of spheroplasting media containing 1 mM $MnCl_2$ and 1 mM $CaCl_2$ and incubated with concanavalin A (25 mg/1600 OD_{600} units) for 15 min on ice. Spheroplasts are pelleted by centrifugation and resuspended at 80 OD_{600} units/mL in cold lysis buffer (0.6 M sorbitol, 50 mM Tris-HCl, pH 7.5) containing carboxyfluorescein (7.5 mg/mL) and lysed in the cold with 25 strokes of pestle A of a Dounce homogenizer. The lysate is centrifuged at 10000*g* for 10 min to remove unbroken cells, nuclei, mitochondria, and cell debris which come in the pellet fraction. Secretory vesicles are collected by centrifugation of supernatant at 100000*g* for 1 h (Beckman Type 50 Ti rotor). These vesicles are further incubated overnight on ice in lysis buffer containing carboxyfluorescein and washed twice by centrifugation at 100000*g* for 1 h at 4 °C prior to water permeability measurements. Secretory vesicle diameter was measured by dynamic light scatter using a DynaPro-801 instrument (Protein Solutions Inc., Charlottesville, VA). Vesicles had an average diameter of 120 ± 22 nm. Protein expression was confirmed by immunoblotting with anti-AQP1 antibody (*3*).

Water Permeability Measurements on Secretory Vesicles. Water transport was measured by stopped-flow fluorescence quenching as previously described (*20*). Using a stopped-

flow fluorimeter (SF.17MV; Applied Photophysics, Leatherhead, U.K.), the vesicles were rapidly shrunk by abruptly exposing the vesicles to a doubling of extravesicular osmolarity causing carboxyfluorescein to self-quench. Extravesicular carboxyfluorescence fluorescence was quenched by adding anti-fluorescence antibody. Data obtained from 8−16 determinations was averaged and fit to single-exponential curves using software provided by Applied Photophysics (*7*). Fitting parameters are then used to calculate the osmotic water permeability (P_f):

$$dV(t)/dt = (P_f)(SAV)(MVW)[(C_{in}/V(t)) - C_{out}]$$

where $V(t)$ is the relative volume as a function of time, SAV is the surface area-to-volume ratio, MVW is the molar volume of water (18 cm^3/mol), and C_{in} and C_{out} are the initial concentrations of total solute inside and outside the vesicle as described (*7*, *27*). Osmolarity was measured by a Wescor vapor pressure osmometer (Wescor Inc., Logon, UT).

Velocity Sedimentation Analyses. Yeast secretory vesicles isolated from 200 mL cultures were solubilized in 1 mL of 2% *N*-lauroylsarcosine containing 50 mM Tris-HCl, pH 7.5, by incubation at room temperature for 1 h and centrifuged at 100000*g* for 1 h to remove unsolubilized material. A 400 μL aliquot of the supernatant was layered over a 4.2 mL 5−20% (w/v) sucrose gradient in the same buffer containing 1% Triton X-100, and spun in a Beckman SW 50.1 rotor for 16 h at 34 000 rpm at 4 °C. Fractions of 200 μL were collected and analyzed by immunoblot. Protein standards (β-amylase, 8.9 S; bovine serum albumin, 4.3 S; carbonic anhydrase, 2.9 S; cytochrome *c*, 1.8 S) were processed similarly (*3*).

Detergent Solubility Studies. Secretory vesicles (5 mg/mL), in a final volume of 1 mL, were incubated in the presence of various detergents for 1 h at room temperature and centrifuged at 100000*g* for 1 h at 4 °C. The presence of AQP1 in supernatant or pellet was determined by immunoblot.

RESULTS

Expression and Water Transport Activity in Oocytes. The possibility that hourglass pore-forming domains in adjacent AQP1 subunits may influence tetramer assembly was approached by constructing a series of tandem dimer cDNAs for functional expression. Dimer cDNAs were formed by splicing *Bam*HI sites at the 3′ end of the K267-Bam AQP1 cDNA and at the 5′ end of the K6-Bam AQP1 cDNA. The resulting cDNA encodes a 530 residue polypeptide (AQP1−AQP1) with an N-terminal subunit (residues 1−267) continuous with a C-terminal subunit (residues 7−269) (*14*). Because of observed differences in complementation exhibited by monomeric AQP1 polypeptides with mutations in corresponding pore-lining residues (*14*), the mutants A73M (loop B) and C189M (loopE) were studied by preparing multiple combinations of tandem dimer constructs (Figure 1 and Table 1).

Complementary RNAs were injected into *X. laevis* oocytes for functional analysis (*6*). Consistent with our previous studies (*14*), AQP1−AQP1 and AQP1−C189S generated comparable levels of 55 kDa protein expression when measured by immunoblot (Figure 2, bottom panel). Likewise, both exhibited high permeabilities ($P_f > 250 \times 10^{-4}$ cm/s)

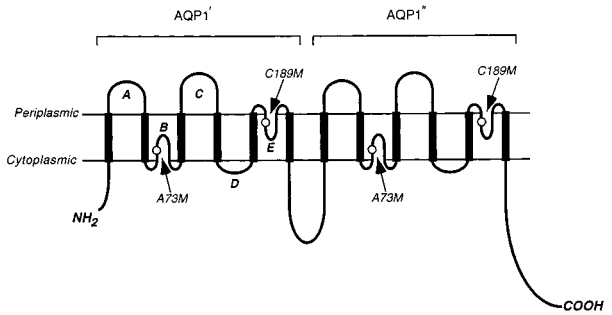

FIGURE 1: Schematic diagram of a AQP1−AQP1 dimer. Two AQP1 monomers joined tail-to-head in tandem are expressed as a single 55 kDa polypeptide. Arrows indicate the positions where site-specific substitutions were introduced.

Table 1: Expression of AQP1 Dimer Polypeptides in Oocytes and Yeast

construct	oocytes	yeast
AQP1−AQP1	+	+
AQP1−C189S	+	+
AQP1−C189M	+	+
AQP1−A73M	+	+
C189M−C189M	−	+
C189M−A73M	+	+
A73M−C189M	−	+
A73M−A73M	−	+

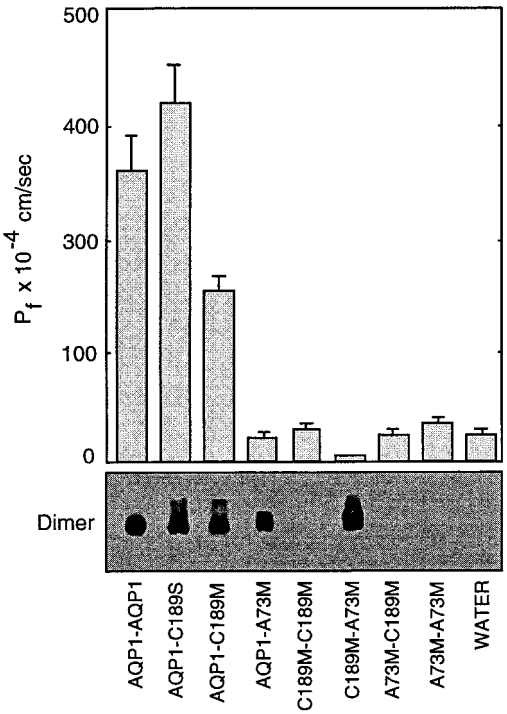

FIGURE 2: Osmotic water permeability (P_f) and protein expression of AQP1 dimer polypeptides in oocytes. The top panel shows the P_f values of oocytes injected with 50 nL of water containing 5 ng of cRNA encoding AQP1−AQP1 or dimers with the indicated site-specific substitutions. P_f values represent the mean and standard deviations from 8−10 oocytes. The bottom panel shows an anti-AQP1 immunoblot of total membranes pooled from 8−10 oocytes and fractionated by SDS−PAGE in a 12% gel.

when measured by the oocyte swelling assay (Figure 2, top panel), whereas control, water-injected oocytes exhibited low water permeability ($< 25 \times 10^{-4}$ cm/s). Recombinants with a wild-type N-terminal subunit joined to a mutant C-terminal subunit (AQP1−A73M and AQP1−C189M) produced com-

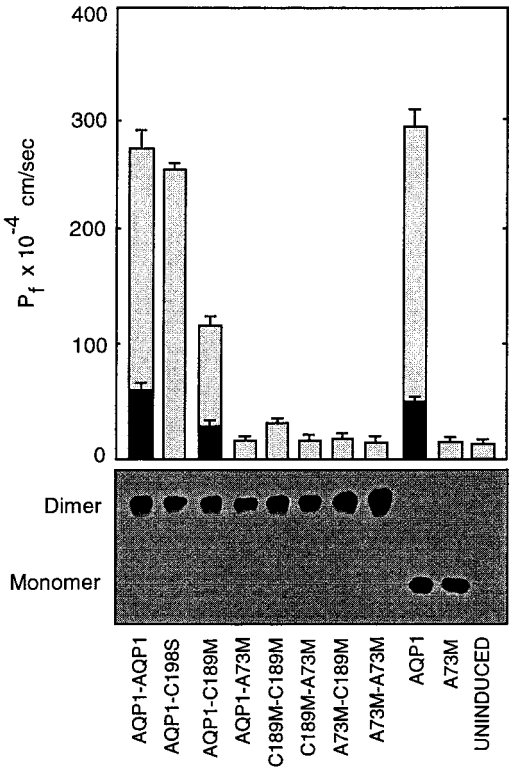

FIGURE 3: Osmotic water permeability (P_f) and protein expression of AQP1 monomer and dimer polypeptides in yeast secretory vesicles. The top panel shows P_f values of secretory vesicles expressing the indicated polypeptides without previous incubation (gray bars) or after 10 min of incubation in 1 mM pCMBS (black bars). P_f values represent the mean and standard deviations of 3−5 determinations. The bottom panel shows an anti-AQP1 immunoblot of 10 μg of expressed proteins from secretory vesicles fractionated by SDS−PAGE in a 12% gel.

parable levels of protein expression, but the AQP1−C189M dimer conferred approximately half the water permeability of AQP1−AQP1, while AQP1−A73M conferred low water permeability comparable to control, water-injected oocytes (Figure 2). When double mutants containing a substitution in each subunit were evaluated, only the C189M−A73M was expressed in levels comparable to AQP1−AQP1: however, the oocytes exhibited low water permeability compared to control oocytes. Injection of oocytes with cRNAs corresponding to the double mutants C189M−C189M, A73M−A73M, and A73M−C189M all failed to produce detectable levels of protein expression and exhibited low water permeabilities (Figure 2).

Expression and Water Transport Activity in Yeast. Since defective membrane trafficking makes the *X. laevis* oocyte expression system uninterpretable for evaluation of some AQP1 mutants, expression in *S. cerevisiae* was employed. Expression of the tandem dimer proteins was evaluated by immunoblot, and water permeability was measured by a stopped-flow spectrophotometer. All of the 55 kDa tandem dimer proteins were found to be abundantly expressed in the yeast system, and the wild-type AQP1 migrated with its expected size of 28 kDa (Figure 3, bottom panel). Secretory vesicles containing the AQP1−AQP1 tandem dimer exhibited osmotic water permeability similar to vesicles containing wild-type AQP1 which is 10−20-fold higher than control vesicles from uninduced yeast (Figure 3, top panel). As in the oocyte studies (described previously), AQP1−C189M exhibited approximately half the osmotic water permeability, while the mutant AQP1−A73M exhibited low water permeability comparable to control vesicles from uninduced yeast. The double mutants C189M−C189M exhibited osmotic water permeability only slightly higher than control vesicles from uninduced yeast, while A73M−C189M, C189M−A73M, and A73M−A73M each exhibited water permeability comparable to control vesicles (Figure 3). Incubation of the vesicles in the mercurial pCMBS inhibited the water channel activity of the wild-type AQP1, AQP1−AQP1, and AQP1−C189M by 70−80%.

Detergent Solubilization and Velocity Gradient Centrifugation of Recombinant Proteins. The native AQP1 protein is known to exist as a tetramer (*3*, *18*, *29*). The partial decrease in water permeability of vesicles containing tandem dimers with a wild-type subunit spliced to a mutant subunit (AQP1−C189M) indicates that the wild-type subunit is still functional, remains pCMBS-inhibitible, and is not perturbed by the mutant subunit. The failure to measure increased water permeability of vesicles containing dimeric proteins containing a wild-type subunit spliced to the other mutant subunit (AQP1−A73M) indicates that the mutant subunit must somehow interfere with the function of the wild-type subunit. To evaluate possible structural defects, the solubilities of yeast vesicle proteins were evaluated with 2% concentrations of detergents: octyl glucoside, Triton X-100, dodecyl maltoside, CHAPS, deoxycholate, and *N*-lauroylsarcosine (Table 2). AQP1, AQP1−AQP1, AQP1−C189M, and C189M−C189M were soluble in each detergent. In contrast, A73M and AQP1−A73M, and C189M−A73M were only soluble in 2% *N*-lauroylsarcosine, a concentration above that used to extract red cell membranes during purification of AQP1 (*3*).

To examine the possibility that these physical differences in protein behavior reflect differences in subunit assembly, the solubilized proteins were evaluated by estimation of sedimentation coefficients by ultracentrifugation in sucrose gradients (5−20%), conditions which previously demonstrated the apparent $s = 5.7$ S for human red cell AQP1 (*3*). The recombinant aquaporin proteins expressed in yeast were solubilized and analyzed by this approach (Figure 4). AQP1 and the wild-type tandem dimer AQP1−AQP1 were found to have major peaks in fractions 9−11, corresponding to an apparent $s \sim 6$ S (tetramers). In contrast, the nonfunctional mutant A73M migrated in earlier fractions 4−7, corresponding to an apparent $s < 3.5$ S (dimers and monomers). AQP1−C189M which was found to retain partial function in both the oocyte system (Figure 2) and yeast vesicle assay (Figure 3) was found to migrate as two peaks—a minor peak in lighter fractions and a major peak coinciding with the heavier fractions. The tandem dimer proteins AQP1−A73M, C189M−A73M, and C189M−C189M which failed to exhibit increased water permeability in yeast vesicles all exhibited mobilities similar to the A73M protein during velocity sedimentation. The tendency of the proteins to form SDS aggregates or their inability to penetrate an SDS−PAGE gel was not observed in these mutants, suggesting that these may not be grossly misfolded.

DISCUSSION

Although numerous studies have been published describing mutations in aquaporin genes, the oocyte expression system

Table 2: Solubility of AQP1 Polypeptides from Yeast Secretory Vesicles in 2% Concentrations of Detergent[a]

construct	octyl glucoside	Triton X-100	dodecyl maltoside	deoxy-cholate	CHAPS	*N*-lauroyl-sarcosine
AQP1	+	+	+	+	+	+
A73M	−	−	−	−	−	+
AQP1−AQP1	+	+	+	+	+	+
AQP1−C189M	+	+	+	+	+	+
AQP1−A73M	−	−	−	−	−	+
C189M−A73M	−	nd	nd	nd	nd	+
C189M−C189M	+	+	+	+	+	+

[a] Soluble (+), insoluble (−), not determined (nd).

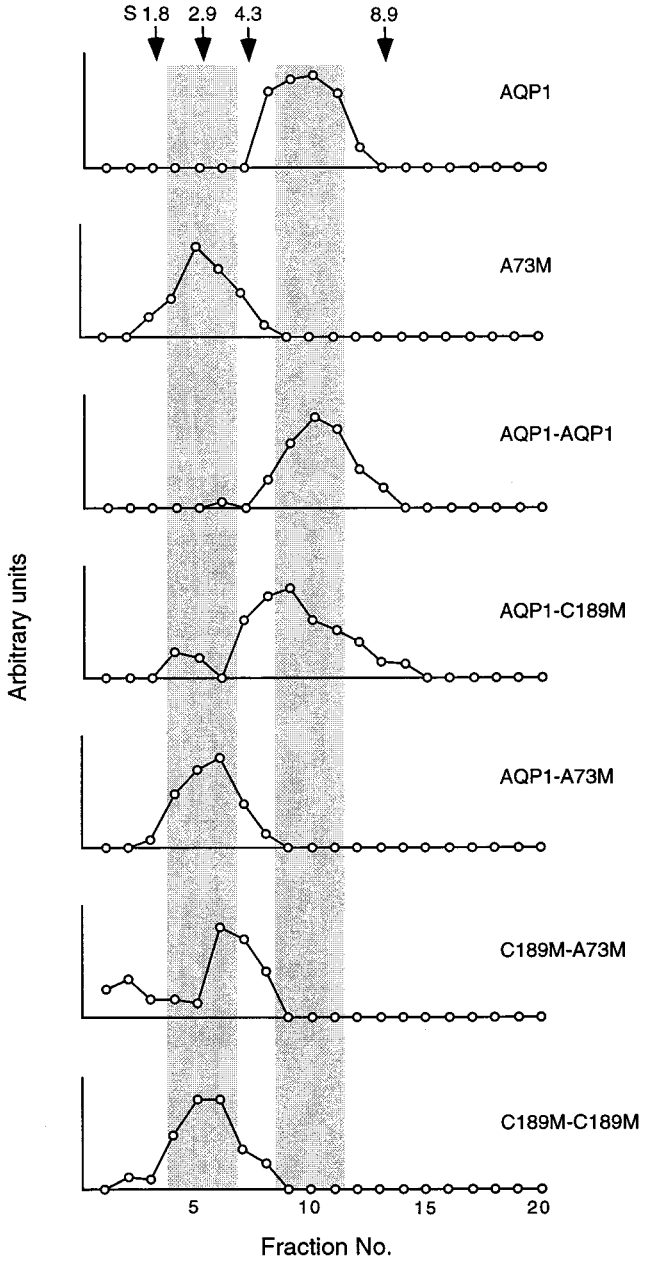

FIGURE 4: Velocity sedimentation profiles of wild-type and site-specific substituted AQP1 monomer and dimer polypeptides from yeast secretory vesicles. Vesicles containing the indicated polypeptides were solubilized in 2% *N*-lauroylsarcosine and centrifuged through 5−20% sucrose gradients (see Materials and Methods). Collected fractions were analyzed by densitometric scanning of anti-AQP1 immunoblots.

permits only limited insight into the behavior of mutant AQP1 polypeptides. Many mutant AQP1 polypeptides traffic to the plasma membrane where they confer osmotic water permeability similar to wild-type AQP1. Rare AQP1 mutants traffic to the membrane but fail to function. Some AQP1 mutants fail to traffic to the cell surface, so the water permeability cannot be assessed, while others are expressed at low levels. The largest reported series of AQP1 recombinants expressed in oocytes showed that most mutations in residues near the NPA motifs in loop B and loop E have low water permeability, presumably because the mutant polypeptides failed to traffic to the oocyte plasma membrane (*14*).

Nevertheless, expression in *X. laevis* oocytes has provided the initial insight into the structure of AQP1 and led to the proposed hourglass model (*14*). Identification of residue Cys-189 in loop E as the Hg^{2+}-sensitive site was made by testing the mutant C189S which had high water permeability but lacked Hg^{2+} inhibition (*11*). Replacement of Cys-189 with larger residues (Tyr, Try, or Met) caused low water permeability. Ala-73 is the loop B residue which corresponds to Cys-189 in loop E, and expression of A73M in oocytes resulted in low water permeability. Expression in temperature-sensitive strains of *S. cerevisiae* that accumulate secretory vesicles (*26*) has previously been used for expression of aquaporins (*20, 21*). Here we employed this system to characterize recombinant aquaporins which could not be functionally analyzed in oocytes, and we confirmed that low water permeability of A73M is an inherent defect in the protein, not simply a problem with membrane trafficking in oocytes.

A series of complementation studies was previously undertaken in oocytes which suggested that loop B and loop E may possibly influence tetramer assembly (*14*). The truncation mutant D237 lacks the C-terminal cytoplasmic domain (site of a presumed targetting signal) but retains the six transmembrane domains and the aqueous pore formed by the overlap of loop B and loop E (*14*). Expression of D237Z in oocytes did not result in high water permeability, due to presumed failure to traffic to the plasma membrane. Expression of the loop B mutants A73M or N76Q failed to increase oocyte water permeability, and when coexpressed with D237Z, both failed to complement. In contrast, coexpression of the loop E mutants C189M or C189W with D237Z led to functional complementation, and formation of mixed oligomers was confirmed by immunoprecipitation (*14*).

The failure of loop B mutants (A73M and N76Q) and the loop E mutant (N192Q) to complement D237Z was previously left unexplained. Chances of a mutant AQP1 associating with a wild-type AQP1 subunit will be greatly increased by expression within tandem dimers. Nevertheless, the

studies reported here demonstrate the failure of tandem dimers including AQP1−A73M to assemble into tetramers. Thus, A73M may interfere with the formation of the hourglass within the individual subunit, but it apparently also leads to misalignment of surrounding contact points between subunits. Despite the functional similarities of residue 73 in loop B and the corresponding residue 189 in loop E, subtle physical differences have been observed. Expression in oocytes of the double mutant A73C/C189S resulted in high water permeability which was Hg^{2+}-inhibitible, but the mutant was less sensitive than wild-type AQP1 to inhibition by Hg^{2+} (*14*). This suggests that both of these residues are located near a critical narrowing of the aqueous pore, but residue 73 is less accessible to Hg^{2+}. Residue 189 may also partially restrict tetramer assembly, since here we found that the mutant dimer C189M−C189M exhibits low water permeability in yeast vesicles and fails to form tetramers.

The challenge is to merge these observations with the structure of AQP1 as established at 6 Å resolution by cryoelectron microscopy (*15*). When the projection is viewed in crosssection, the six α-helical transmembrane (TM) domains are tilted at ∼20° and form a right-handed bundle. Moreover, when the projection is viewed from the extracellular surface, the TMs are arranged counterclockwise around a central density believed to represent overlapping loop B and loop E. Although structural assignments are not definite, loops B and E do not appear to represent contact sites between subunits, and loop B appears as a narrow, kinked structure, whereas loop E resembles a broader funnel. TM1 and TM3 in adjacent subunits appear to make contact, as do TM4 and TM6. The studies reported here indicate that a single amino acid substitution in loop B may lead to misalignment of the flanking α-helical transmembrane domains (TM2 and TM3). Thus, A73M may perturb the orientation of TM3 which no longer fits well with TM1 in the adjacent subunit, even if joined as a dimer in a single 55 kDa polypeptide (AQP1−A73M). The corresponding substitution in loop E was less critical to tetramer formation, since AQP1−C189M resulted in tetramers with partial water permeability. Nevertheless, when this substitution occurs as the dimer C189M−C189M, tetramer assembly is not achieved. Although the detailed structural explanations for these observations are still speculative, together the studies reported here indicate that the domains responsible for AQP1 water permeation are also critical to subunit assembly.

ACKNOWLEDGMENT

We thank Dr. Rajini Rao for sharing resources and providing useful discussions. We thank Gregory M. Preston, Kushal Bhakta, and Matthew R. T. Hall for their participation in preparing cDNA constructs and providing valuable suggestions. Access to the stopped-flow spectrophotometer and operational assistance were provided by J. P. Froehlich and P. Heller (National Institute of Aging, NIH, Baltimore, MD). Core oocyte facilities were provided by Wm. B. Guggino, Department of Physiology, Johns Hopkins School of Medicine.

REFERENCES

1. Finkelstein, A. (1987) in *Water Movement Through Lipid Bilayers, Pores, and Plasma Membranes. Theory and Reality*, John Wiley and Sons, Inc., New York.
2. Denker, B. M., Smith, B. L., Kuhajda, F. P., and Agre, P. (1988) *J. Biol. Chem. 263*, 15634−15642.
3. Smith, B. L., and Agre, P. (1991) *J. Biol. Chem. 266*, 6407−6415.
4. Nielsen, S., Smith, B. L., Christensen, E. I., Knepper, M. A., and Agre, P. (1993) *J. Cell Biol. 120*, 371−383.
5. Nielsen, S., DiGiovanni, S. R., Christensen, E. I., Knepper, M. A., and Harris, H. W. (1993) *Proc. Natl. Acad. Sci. U.S.A. 90*, 11663−11667.
6. Preston, G. M., Carroll, T. P., Guggino, W. B., and Agre, P. (1992) *Science 256*, 385−387.
7. Zeidel, M. L., Ambudkar, S. V., Smith, B. L., and Agre, P. (1992) *Biochemistry 31*, 7436−7440.
8. Agre, P., Bonhivers, M., and Borgnia, M. J. (1998) *J. Biol. Chem. 273*, 14659−14662.
9. Preston, G. M., and Agre, P. (1991) *Proc. Natl. Acad. Sci. U.S.A. 88*, 11110−11114.
10. Park, J. H., and Saier, M. H. (1996) *J. Membr. Biol. 153*, 171−180.
11. Preston, G. M., Jung, J. S., Guggino, W. B., and Agre, P. (1993) *J. Biol. Chem. 268*, 17−20.
12. Zhang, R., van Hoek, A. N., Biwersi, J., and Verkman, A. S. (1993) *Biochemistry 32*, 2938−2941.
13. Preston, G. M., Jung, J. S., Guggino, W. B., and Agre, P. (1994) *J. Biol. Chem. 269*, 1668−1673.
14. Jung, J. S., Preston, G. M., Smith, B. L., Guggino, W. B., and Agre, P. (1994) *J. Biol. Chem. 269*, 14648−14654.
15. Walz, T., Hirai, T., Murata, K., Heymann, J. B., Mitsuoka, K., Fujiyoshi, Y., Smith, B. L., Agre, P., and Engel, A. (1997) *Nature 387*, 624−627.
16. Li, H., Lee, S., and Jap, B. K. (1997) *Nat. Struct. Biol. 4*, 263−265.
17. Cheng, A., van Hoek, A. N., Yeager, M., Verkman, A. S., and Mitra, A. K. (1997) *Nature 387*, 627−630.
18. Verbavatz, J. M., Brown, D., Sabolic, I., Valenti, G., Ausiello, D. A., van Hoek, A. N., Ma, T., and Verkman, A. S. (1993) *J. Cell Biol. 123*, 605−618.
19. Shi, L. B., Skach, W. R., and Verkman, A. S. (1994) *J. Biol. Chem. 269*, 10417−10422.
20. Coury, L. A., Mathai, J. C., Prasad, G. V. R., Brodsky, J. L., Agre, P., and Zeidel, M. L. (1998) *Am. J. Physiol. 43*, F34−F42.
21. Lagrée, V., Pellerein, I., Hubert, J.-F., Tacnet, F., Le Cahérec, F., Roudier, N., Thomas, D., Gouranton, J., and Deschamps, S. (1998) *J. Biol. Chem. 273*, 12422−12426.
22. Zhang, R. B., Logee, K. A., and Verkman, A. S. (1990) *J. Biol. Chem. 265*, 15375−15378.
23. Wall, D. A., and Patel, S. (1989) *J. Membr. Biol. 107*, 189−201.
24. Laemmli, U. K. (1970) *Nature 227*, 680−685.
25. Davis, J. Q., and Bennett, V. (1984) *J. Biol. Chem. 259*, 1874−1881.
26. Nakamoto, R. K., Rao, R., and Slayman C. W. (1991) *J. Biol. Chem. 266*, 7940−7949.
27. Priver, N. A., Rabon, E. C., and Zeidel, M. L. (1993) *Biochemistry 32*, 2459−2468.
28. Zeidel, M. L., Nielsen, S., Smith, B. L., Ambudkar, S. V., Maunsbach, A. B., and Agre, P. (1994) *Biochemistry 33*, 1606−1615.
29. Waltz, T., Smith, B. L., Zeidel, M. L., Engel, A., and Agre, P. (1994) *J. Biol. Chem. 269*, 1583−1586.

BI9823683